REPORT

Bi-allelic Variants in *RALGAPA1* Cause Profound Neurodevelopmental Disability, Muscular Hypotonia, Infantile Spasms, and Feeding Abnormalities

Matias Wagner,[1,2,3,18,*] Yuliya Skorobogatko,[4,18] Ben Pode-Shakked,[5,6,18] Cynthia M. Powell,[7]
Bader Alhaddad,[1] Annette Seibt,[8] Ortal Barel,[9] Gali Heimer,[6,10] Chen Hoffmann,[6,11]
Laurie A. Demmer,[12] Yezmin Perilla-Young,[7] Marc Remke,[13] Dagmar Wieczorek,[14]
Tharsini Navaratnarajah,[8] Peter Lichtner,[2] Dirk Klee,[15] Hanan E. Shamseldin,[16] Fuad Al Mutairi,[17]
Ertan Mayatepek,[8] Tim Strom,[1] Thomas Meitinger,[1] Fowzan S. Alkuraya,[16] Yair Anikster,[5,6]

Q1 Alan R. Saltiel,[4] and Felix Distelmaier[8,*]

Ral (Ras-like) GTPases play an important role in the control of cell migration and have been implicated in Ras-mediated tumorigenicity. Recently, variants in *RALA* were also described as a cause of intellectual disability and developmental delay, indicating the relevance of this pathway to neuropediatric diseases. Here, we report the identification of bi-allelic variants in *RALGAPA1* (encoding Ral GTPase activating protein catalytic alpha subunit 1) in four unrelated individuals with profound neurodevelopmental disability, muscular hypotonia, feeding abnormalities, recurrent fever episodes, and infantile spasms (the latter as part of West syndrome). Dysplasia of corpus callosum with focal thinning of the posterior part and characteristic facial features appeared to be unifying findings. RalGAPA1 was absent in the fibroblasts derived from two affected individuals suggesting a loss-of-function effect of the *RALGAPA1* variants. Consequently, RalA activity was increased in these cell lines, which is in keeping with the idea that RalGAPA1 deficiency causes a constitutive activation of RalA. Additionally, levels of RalGAPB, a scaffolding subunit of the RalGAP complex, were dramatically reduced, indicating a dysfunctional RalGAP complex. Moreover, RalGAPA1 deficiency clearly increased cell-surface levels of lipid raft components in detached fibroblasts, which might indicate that anchorage-dependence of cell growth signaling is disturbed. Our findings indicate that the dysregulation of the RalA pathway has an important impact on neuronal function and brain development. In light of the partially overlapping phenotype between *RALA*- and *RALGAPA1*-associated diseases, it appears likely that dysregulation of the RalA signaling pathway leads to a distinct group of genetic syndromes that we suggest could be named RALopathies.

The Ral guanine nucleotide exchange factor (RalGEF)/Ral GTPase cascade is one of three major downstream pathways that become activated upon Ras signaling. The others include the Raf/mitogen-activated protein kinase (MAPK) cascade and the phosphoinositide 3-kinase (PI3K)-dependent phosphoinositide pathway.[1] *RALGAPA1* (previously referred to as *TULIP1* or *GARNL1* [MIM: 608884]) encodes the catalytic subunit of Ral GTPase-activating protein (GAP) complex for two highly related small G proteins, RalA and RalB.[1,2] Ral proteins draw significant research interest as promising cancer drug targets downstream of Ras.[3,4] The role of RalA in normal cell physiology centers around the regulation of intracellular-vesicle trafficking. RalA mediates post-Golgi vesicle trafficking toward the plasma membrane by rearranging the cytoskeleton and via its interaction with the tethering complex exocyst, which positions vesicles for docking and fusion at the plasma membrane.[5,6] Thus, RalA is implicated in cellular processes, which depend on directional membrane trafficking, such as cell migration, establishment of cell polarity, neuronal polarity, and ciliogenesis. Consequently, RalA is essential for normal brain development. *Rala*-null mouse embryos display exencephaly, which recently has been classified as ciliopathy, between embryonic day 10.5 (E10.5) and E19.5.[7]

RalA activity is regulated in response to extracellular cues. For example, RalA mediates the delivery of vesicles that contain the glucose transporter GLUT4 toward the plasma membrane in adipocytes treated with insulin and also mediates the formation of lamellipodia in fibroblasts

[1]Institute of Human Genetics, Technical University München, 81675 Munich, Germany; [2]Institute of Human Genetics, Helmholtz Zentrum München, 85764 Neuherberg, Germany; [3]Institute for Neurogenomics, Helmholtz Zentrum München, 85764 Neuherberg, Germany; [4]Department of Medicine, University of California, San Diego School of Medicine, La Jolla, CA 92093, USA; [5]Metabolic Disease Unit, Edmond and Lily Safra Children's Hospital, Sheba Medical Center, 52621 Tel-Hashomer, Israel; [6]Sackler Faculty of Medicine, Tel-Aviv University, 6997801 Tel-Aviv, Israel; [7]Department of Pediatrics, University of North Carolina at Chapel Hill School of Medicine, Chapel Hill, NC, 27599, USA; [8]Department of General Pediatrics, Neonatology and Pediatric Cardiology, University Children's Hospital, Medical Faculty, Heinrich-Heine-University, 40225 Düsseldorf, Germany; [9]Genomics Unit, Sheba Cancer Research Center, Sheba Medical Center, 52621 Tel-Hashomer, Israel; [10]Pediatric Neurology Unit, Edmond and Lily Safra Children's Hospital, Sheba Medical Center, 52621 Tel-Hashomer, Israel; [11]Department of Radiology, Sheba Medical Center, 52621 Tel-Hashomer, Israel; [12]Medical Genetics, Atrium Health Levine Children's Hospital, Charlotte, NC, 28203, USA; [13]Department of Pediatric Oncology, Hematology, and Clinical Immunology, Medical Faculty, University Hospital Düsseldorf, 40225 Düsseldorf, Germany; [14]Institute of Human Genetics, Medical Faculty, Heinrich Heine University, 40225 Düsseldorf, Germany; [15]Department of Diagnostic and Interventional Radiology, Heinrich-Heine University, 40225 Düsseldorf, Germany; [16]Department of Genetics, King Faisal Specialist Hospital and Research Center, 12713 Riyadh, Saudi Arabia; [17]Division of Genetics, Department of Pediatrics, King Saud bin Abdulaziz University for Health Sciences, King Abdulaziz Medical City, 12713 Riyadh, Saudi Arabia
[18]These authors contributed equally to this work
*Correspondence: Matias.Wagner@mri.tum.de (M.W.), felix.distelmaier@med.uni-duesseldorf.de (F.D.)
https://doi.org/10.1016/j.ajhg.2020.01.002.

treated with TNFα.[8,9] As is true for a typical G protein, RalA activity depends on its nucleotide-binding status. Binding to GTP activates RalA, whereas binding to GDP renders RalA inactive.[10] Thus, RalA is regulated by factors that facilitate nucleotide exchange (guanine exchange factors [RalGEFs]) or GTP hydrolysis (RalGAP). In its basal state, RalA is maintained in an inactive GDP-bound form by the RalGAP complex and can be activated either by RalGEF (as it happens downstream of Ras) or by the inactivation of RalGAP (as was described for insulin signaling).[10] The RalGAP complex is a heterodimer of a catalytic subunit, either RalGAPA1 or RalGAPA2 (the expression of which is cell-type-specific), and a scaffolding subunit, RalGAPB.[2] It has been demonstrated in several mouse models that the loss of either RalGAP subunit results in constitutive activation of Ral proteins, and physiological outcomes are highly cell-type- and development-stage-specific. It is important to note that the ability to cycle between GTP- and GDP-bound states might be important for RalA function.[10] Thus, although constitutive RalA activation might facilitate certain signaling cascades, it might disrupt the others.

Although the Ral GTPase pathway is well known in cancer biology, its implication in Mendelian disorders has yet to be elucidated. Pathogenic variants in *RALA* (MIM: 179550) have been identified as a cause of an autosomal-dominant inherited syndrome typified by speech and motor delays, intellectual disability, early-onset epilepsy, short stature, facial dysmorphism, and finger and toe abnormalities (e.g., long fingers with extensible joints, finger overlap, and toe clinodactyly).[11] *RALGAPA1* is ubiquitously expressed; the highest expression levels are in the brain, ovaries, and uterus (GTEx portal with dbGaP accession phs000424.v7.p2 on 02/07/2019). *RALGAPA1* has been suggested as a candidate gene for neurodevelopmental disorders because magnetic resonance tomography imaging (MRI) identified microdeletions including *RALGAPA1* in individuals with developmental delay, microcephaly, seizures, muscular hypotonia, and mild brain atrophy, and *RALGAPA1* was the only deleted gene with high expression in the brain.[12,13] A morpholino oligonucleotide knockdown of the homolog *tulip1* in a zebrafish model resulted in severe developmental impairment of the brain and comparably mild abnormalities of the whole body.[12]

Here, by identifying bi-allelic variants in *RALGAPA1* in four unrelated families, we establish that the loss of *RALGAPA1* disrupts the RalGAP complex, leads to constitutive RalA activation, and causes a severe neurodevelopmental disease with profound muscular hypotonia, infantile spasms, and feeding difficulties.

Legal guardians of all individuals investigated gave written informed consent for genetic testing and functional studies from tissue material (families A and B). Permission to include clinical photographs was obtained. The study was performed according to the declaration of Helsinki. The local ethical committees at the Heinrich-Heine-University Düsseldorf (#4957), the Technical University in Munich (#5360/12S), King Faisal Specialist Hospital and Research Center (RAC #2080006), and the Sheba Medical Center (#7786-10-SMC) approved the genetic studies and the studies on tissue samples derived from individuals 1 and 2, where applicable.

The clinical phenotype of the affected individuals is summarized in Table 1. Detailed case reports can be found in the Supplemental Information.Pedigrees and clinical images are depicted in Figure S1 and Figure 1, respectively.

All individuals were born after uneventful pregnancies. Only one child was born preterm. Birth parameters were normal in two individuals, and two children were born small for gestational age. All four children presented with respiratory distress requiring transient non-invasive ventilation directly after birth. One child required a tracheostomy as a result of persistent respiratory problems. Congenital profound muscular hypotonia was a unifying clinical feature. During the first year of life, three individuals had frequent episodes of high fever. A dysregulation of central temperature control was suspected. In two individuals, recurrent viral infections were noted, but there were no abnormalities on immunologic work-up. In one child, hypohidrosis was diagnosed. All individuals had feeding abnormalities requiring tube feeding. Infantile spasms starting between the ages of 8 and 12 months were observed in three out of four children. In this context, it should be noted that the only child without clinical evidence of epilepsy is still very young (8 months at last followup appointment). Seizures responded to ACTH treatment in one child, and two children suffered from drug-resistant epilepsy. Profound developmental delay was observed in all children, none of whom reached any major developmental milestones. Brain MRIs in the affected individuals revealed dysplasia of the corpus callosum; focal thinning of the posterior part (splenium) was a unifying CNS finding (Figure 1 and Figure S2). In addition, a wide spectrum of unspecific abnormalities, including gray-matter heterotopias, ectopic posterior pituitary, signal abnormalities in basal ganglia, and stratum subependymale, was observed (see Figure S3). Only one child showed signs of global brain atrophy (Figure 1). Interestingly, moderate dysmorphic facial features were observed in all of the children. They had a rather consistent phenotype of upslanting palpebral fissures, mild epicanthus, a short nose with a flattened nasal bridge, and slightly anteverted nares (see Figure 1). The oldest child is now 5 years old and is severely disabled. He is unable to sit, crawl, or pull up. Head control is still inadequate, and truncal muscle tone is profoundly reduced. He did not acquire language, and he never interacted with his environment.

Exome sequencing (ES) was performed at four clinical sites in Munich, Tel-Aviv, Chapel Hill, and Riyad. For family A, trio ES was performed with the Sure Select Human All Exon kit V5 (index individual) and V6 (parents; Agilent) for exome enrichment and a HiSeq2500 (index individual) and HiSeq4000 (parents) system (Illumina) for sequencing. The average read depth was 131×. Reads were aligned to the UCSC human reference assembly (hg19) with the

Table 1. Clinical Characteristics of Individuals with *RALGAPA1* Variants

Family	Family A	Family B	Family C	Family D
ID	**Individual 1**	**Individual 2**	**Individual 3**	**Individual 4**
Age at last examination	4 1/2 years	8 months	18 months	17 months
Gender	male	female	male	male
Genome molecular analysis	exome sequencing	exome sequencing	exome sequencing	exome sequencing
Variant (NM_194301.4)	c.3227A>G;1126C>T, (p.Asn1076Ser;Arg376*)	c.4992del;4992del, (p.Phe1664Leufs*11; Phe1664Leufs*11)	c.610G>T;610G>T, (p.Glu204*;Glu204*)	c.5732C>G);(5732C>G), (p.Ser1911*;Ser1911*)
Pathogenicity	pathogenic	pathogenic	pathogenic	pathogenic
Q23 Familial History with Regard to the Perinatal Period				
Ancestry	German	Palestinian	German and Irish	Saudi
Consanguinity	no	yes	no	yes
Pregnancy	unremarkable	unremarkable	poor maternal weight gain	preterm delivery
Prematurity	no	no	no	born at 34 weeks
Perinatal period	neonatal respiratory distress	neonatal respiratory distress	neonatal respiratory distress	neonatal respiratory distress
Growth Parameters				
Birth length	56 cm (97th centile)	N/A	45.5 cm (5th centile)	43 cm (<5th centile)
Birth weight	3,875 g (79th centile)	3,000 g (20th centile)	2,240 g (5th centile)	2,115 g (<5th centile)
Head circumference	36.5 cm (93th centile)	N/A	33.5 cm (13th centile)	33.5 cm (10th centile)
Age at examination (y)	4 1/2 years	3 months	18 months	17 months
Current height	111 cm (75th centile)	51 cm (<1st centile)	78.1 cm (6th centile)	75 cm (5th centile)
Current weight	16.4 kg (25th centile)	2.9 kg (<1st centile)	9.52 kg (7th centile)	12.5 kg (75th centile)
Current head circumference	51.5 cm (52th centile)	35 cm (<1st centile)	46.8 cm (7th centile)	48 cm (37th centile)
Motor development	severely delayed	severely delayed	severely delayed	severely delayed
Speech development	none	none	none	none
Neurological Findings				
Muscle tone	profound muscular hypotonia	profound muscular hypotonia	profound muscular hypotonia	profound muscular hypotonia
Head control	poor	poor	poor	poor
Spasticity	no	yes	no	yes
UL/LL tendon reflexes	reduced/reduced	reduced/reduced	reduced/reduced	increased
Seizures	infantile spasms	no	infantile spasms	infantile spasms
Brain MRI	focal thinning of corpus callosum, gray matter heterotopias	focal thinning of corpus callosum, thin pituitary stalk, global brain atrophy	focal thinning of corpus callosum, ectopic pituitary	focal thinning of corpus callosum
Skin findings	dry skin and hypohidrosis	none	none	none
Ophthalmologic findings	bilateral cataract	none	cortical vision impairment (no cataracts)	suspected cortical vision impairment (not confirmed)
General Clinical Findings				
Heart	normal	normal	normal	mild tricuspid valve regurgitation and mild mitral valve regurgitation.
Lungs	normal	tracheostomy	laryngomalacia, oxygen by nasal canula during sleep	recurrent apnea, tracheomalacia with intermittent stridor

(Continued on next page)

Table 1. *Continued*

Family	Family A	Family B	Family C	Family D
ID	Individual 1	Individual 2	Individual 3	Individual 4
Gastrointestinal tract	feeding difficulties, gastrostomy tube	feeding difficulties, nasogastric tube	feeding difficulties, gastrostomy tube	feeding difficulties, gastrostomy tube, gastro-esophageal reflux
Urinary tract	bilateral vesicoureteric reflux grade II	normal	normal	vesicoureteric reflux, right grade III / IV and left grade III
Recurrent fever / frequent viral infections	yes	yes	no	yes
Limbs	drop foot	normal	soft tissue syndactyly of fingers 3 and 4 bilaterally, partial syndactyly of toes 2, 3, and 4 on the right foot	normal
Craniofacial features	thick eyebrows, deep-set eyes, short nasal bridge with anteverted nares, large mouth with prominent lower lip, protruding tongue	bushy eyebrows and a low anterior hairline	flat occiput and brachycephaly, high anterior hair line with frontal balding, tall forehead, full cheeks, medial eyebrow flare, left epicanthal fold, pointed superior helices of ears, upturned nasal tip	horizontal eyebrows, low-set ears, depressed nasal bridge, and large mouth with prominent lips, and slight retrognathia
Additional clinical findings	gingival hyperplasia	mild hepatomegaly	No	gingival hyperplasia

Abbreviations are as follows: y = year; n/a = not assessed; UL = upper limb; LL = lower limb; and MRI = magnetic resonance imaging.

Burrows-Wheeler algorithm (BWA v.0.5.9). More than 98% of the target sequences were covered to a read depth of at least 20×. Single-nucleotide variants (SNVs) as well as small insertions and deletions were detected with SAMtools v.0.1.19. In-house custom Perl scripts were used for variant annotation.

In family B, trio ES was performed with the Sure Select Human All Exon Kit V6 on a HiSeq2500 sequencing machine (Illumina). Reads were aligned to the UCSC human reference assembly (hg19) with the BWA-MEM algorithm (BWA v.0.7.15). Variants were called with GATK variant caller version 3.8; best practices as recommended by the Broad Institute were used.[14] Variant annotation was performed with KGGSeq.[15]

For family C, trio ES was done on a clinical basis through GeneDx with XomeDxPlus. A *RALGAPA1* homozygous variant was identified but classified as a variant of uncertain significance because no disease was known to be associated with it at that time. 100% of the coding region was covered for this gene at a minimum of 10×, with no indication of a multi-exon deletion or duplication involving this gene.

For family D, index-only ES was performed in parallel with array-based autozygosity mapping as described before.[16]

We filtered for homozygous and compound-heterozygous variants with a minor-allele frequency <0.1% in our in-house database of 15,000 individuals as well as for *de novo* variants that had a minor-allele frequency <0.01%.

A search for bi-allelic variants in family A identified changes in six genes (Table S1), whereas a filter for *de novo* variants did not identify protein altering variants. Among the biallelic variants, variants in *NEB* and *BRCA1*

were associated with autosomal recessive inherited conditions and were classified as variants of uncertain significance. Because there was no phenotypic overlap between the condition of our index individual and previously published individuals these variants were considered to not be associated with the child's condition. Of the remaining variants, only the compound-heterozygous variants in *RALGAPA1* (NM_194301.4) were predicted to result in a loss of function c.3227A>G(p.Asn1076Ser) and c.1126C>T(p.Arg376*). The parents were heterozygous carriers for one of the variants each. Variants were confirmed by Sanger sequencing in the index individual and his parents (Figure S1).

We next sought to identify further families with bi-allelic variants in *RALGAPA1* by using the web-based collaboration platform GeneMatcher.[17] We identified additional individuals who came from three unrelated families and had an overlapping phenotype and bi-allelic loss-of-function variants in *RALGAPA1* in Israel (family B), the USA (family C), and Saudi Arabia (family D, Figure 1). In family B, a homozygous frameshift variant, c.4992delT(p.Phe1664Leufs*11), was detected; in family C, the homozygous nonsense variant c.610G>T(p.Glu204*) was detected.

In family D, the combination of ES and array-based homozygosity mapping revealed a homozygous nonsense variant, c.5732C>G(p.Ser1911*), within an autozygosity block (see Figure S4) that is unique to the affected individuals. Additional information on the *RALGAPA1* variants can be found in Table S2.

To further support the relevance of *RALGAPA1* variants, we used living skin fibroblasts derived from the affected
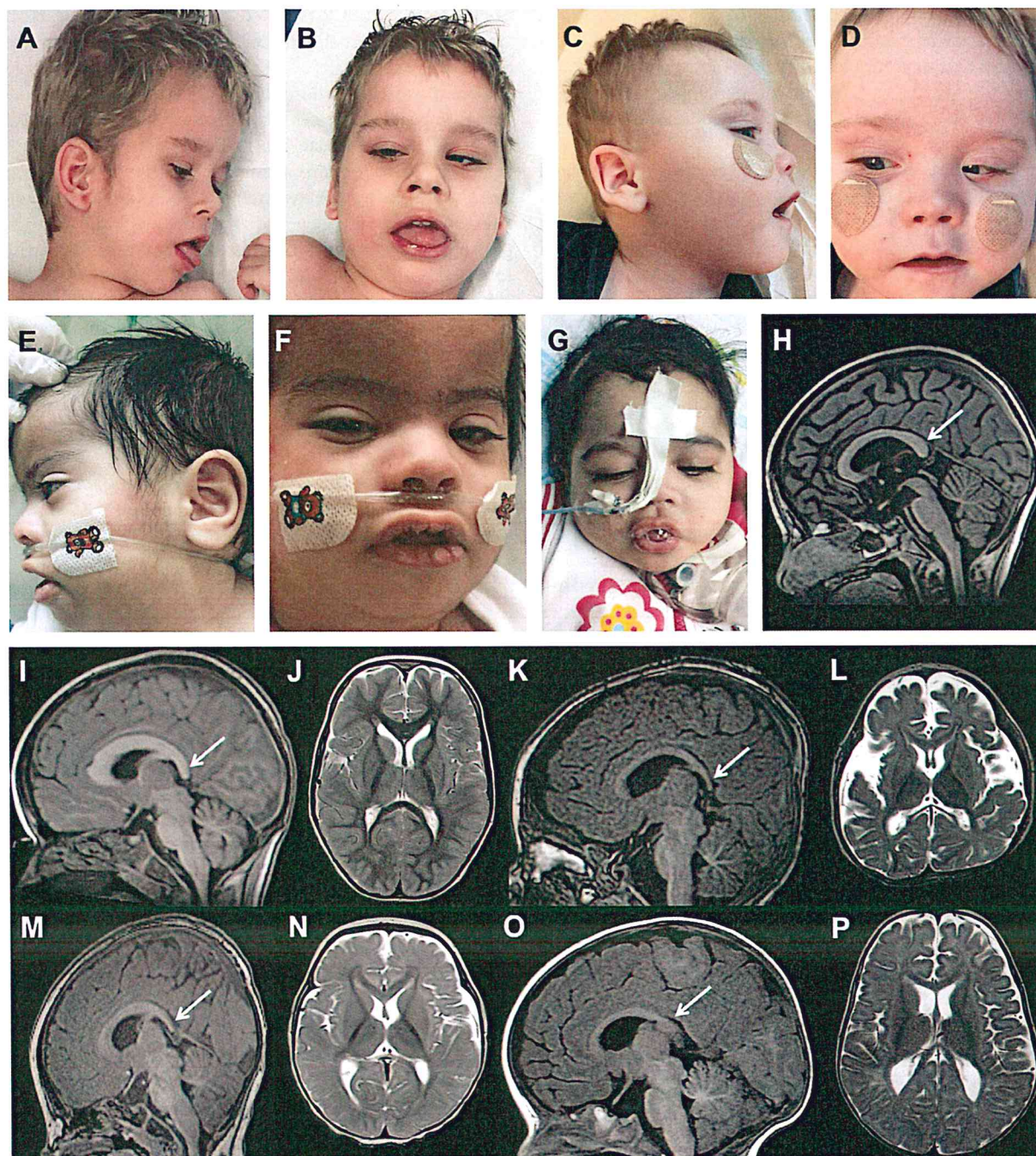
Figure 1. Clinical Details of Affected Individuals

(A–G) Clinical photographs of individuals with pathogenic variants in *RALGAPA1*. (A and B) Individual 1 at the age of 4 $^1/_2$ years. (C and D) Individual 3 at the age of 18 months. (E and F) Individual 4 at the age of 17 months. (G) Individual 2 at the age of 8 months. All children suffered from severe developmental disability with profound muscular hypotonia and feeding abnormalities. Facial features included upslanting palpebral fissures, mild epicanthus, a short nose with a flattened nasal bridge, and slightly anteverted nares.

(H) Brain MRI image (T1-weighted sagittal view) of a healthy individual at the age of 4 1/2 years. The white arrow indicates the posterior part (splenium) of the corpus callosum.

(I–P) Brain MRI images of individuals with bi-allelic variants in *RALGAPA1* (T1-weighted sagittal as well as T2-weighted axial views). (I and J) Individual 1 (age 4 1/2 years). (K and L) Individual 2 (age 8 months). (M and N) Individual 3 (age 10 months). (O and P) Individual 4 (age 8 months). Of note, in all individuals with pathogenic variants in *RALGAPA1*, a moderate dysplasia of the corpus callosum with focal thinning of the posterior part was detectable (white arrows; compare with normal findings in panel [H]). Further details (including age-related normal values) regarding this finding are depicted in Figure S2. In addition, individual 2 showed global brain atrophy (L). Other variable/unspecific CNS abnormalities in individuals with RalGAPA1 deficiency are depicted in Figure S3.

individuals from families A and B. Cell lines were cultured in Dulbecco's modified Eagle's medium (DMEM; life technologies) supplemented with 10% fetal bovine serum (FBS)(Life Technologies) and 1% penicillin-streptomycin (Life Technologies) at 37°C in a humidified atmosphere of 5% CO_2.

For immunoblotting, whole-cell lysates were prepared with cell-lysis reagent CelLyticM (Sigma-Aldrich). A monoclonal antibody against RalGAPA1 (rabbit; 1:3000; EPR13592-38; Abcam) was used. GAPDH served as a loading marker (mouse; 1:4000; Thermo Fisher Scientific; AM 4300, USA). BM chemiluminescence blotting substrate (Roche) was used for visualization. Methodological details can be also found in the Supplemental Information. As depicted in Figure 2, a RalGAPA1 protein signal was nearly absent in fibroblasts of affected individuals, suggesting a loss-of-function effect in the investigated cell lines. To determine whether the variants result in nonsense-mediated decay (NMD), we additionally performed qRT-PCR for *RALGAPA1* expression for individual 1, and this analysis revealed a reduction to 54% of the transcriptional level (Figure S5). This indicates that transcripts with the nonsense variant undergo NMD, whereas the missense variant is expressed, and reduced protein levels are rather a consequence of protein instability.

As a next step, we aimed to gain further insight into the functional consequences of RalGAPA1 deficiency. Of note, the RalGAP complex facilitates GTP hydrolysis on RalA and thus converts RalA into an inactive GDP-bound form. The loss of RalGAP subunits in mice results in constitutively active GTP-bound RalA.[18] This can be exemplified by the deletion of the catalytic subunit RalGAPA2 in the bladder or RalGAPA1 in muscles, as well as the deletion of scaffolding subunit RalGAPB in adipose tissue.[8,18,19] Thus, we tested RalA activation status in human fibroblasts with RalGAPA1 deficiency. For RalA activity measurements, the fibroblasts were starved in FBS-free media and then in PBS. Fresh cell lysates were used for GTP-bound RalA pulldown with RalBP1 beads (Millipore) according to the manual. Samples were diluted in SDS sample buffer with 50 mM DTT, boiled for 5 min, resolved on SDS-PAGE, and transferred to nitrocellulose membranes (Bio-Rad). Individual proteins were detected with the specific antibodies and visualized on film via horseradish-peroxidase–conjugated secondary antibodies and Western Lightning Enhanced Chemiluminescence (Perkin Elmer Life Sciences). Further details are explained in the Supplemental Material and Methods.

In fibroblasts with RalGAPA1 deficiency, RalA activity was increased in comparison to that in control fibroblasts (Figure 2). This finding is in line with the idea that RalGAPA1 deficiency causes constitutive activation of RalA. Additionally, protein levels of RalGAPB, a scaffolding subunit of RalGAP complex, were dramatically reduced in samples without the RalGAPA1 subunit, indicating a dysfunctional RalGAP complex and the necessity of RalGAPA1 for RalGAPB stability. *RALGAPB* expression

analysis via RT-qPCR revealed no downregulation at the transcriptional level, supporting this hypothesis (see Figure S6).

Constitutive activation of the RalA pathway might have important consequences for cell physiology. Importantly, it has been shown that constitutively active RalA retains lipid-raft microdomains in detached cells at the plasma membrane and promotes anchorage-independent growth signaling.[20] It was suggested that this mechanism might play a role in tumor and metastasis formation. To further investigate this aspect in individuals with RalGAPA1 deficiency, we analyzed the localization of lipid-raft components in detached fibroblasts by using the fluorescence marker CTxB-Alexa 594 (for details, see Supplemental Information). Of note, CTxB (cholera toxin B subunit) constitutes the membrane-binding subunit of cholera toxins and serves as a well-established marker of lipid rafts.[21] CTxB Alexa 594 cell-surface fluorescence was visualized by ZEISS ApoTome imaging, and quantitative data were obtained by fluorescence-activated cell sorting (FACS) analysis. As depicted in Figure 2, fibroblasts with variants in *RALGAPA1* retained significantly higher levels of surface lipid-raft components than did several control cell lines. Raw data that were used for quantification can be found in Figure S7. FACS analysis of CTxB-stained fibroblasts confirmed these results with a shift toward higher fluorescence intensity, indicating plasma membrane retention of lipid rafts in RalGAPA1-deficient fibroblasts (see also Figure S8). This finding is in agreement with previous research and indicates that cell-growth signaling might be altered in individuals with RalGAPA1 deficiency.[20]

Taken together, the experiments described above confirmed a loss-of-function character of the *RALGAPA1* variants and are in line with an autosomal-recessive inheritance pattern. Given the loss-of-function nature of the variants we describe here and the strikingly consistent associated phenotype, we conclude that the loss of RalGAPA1 in the individuals reported here is most likely responsible for the observed clinical abnormalities. This hypothesis is strengthened by the gnomAD gene-constraint metrics showing a depletion of loss-of-function and missense variants (observed/expected ratio of loss-of-function variants in *RALGAPA1* = 0.12; 0.69 for missense variants).[22] This finding indicates that *RALGAPA1* is a disease-associated gene. In light of the constraint metrics, the identification of one missense variant in our study group suggests that both loss-of-function and missense variants can cause disease.

Regarding the functional consequences of RalGAPA1 deficiency, it is suggestive that alterations in intracellular trafficking downstream of constitutively active RalA and possibly RalB are involved in disease pathophysiology. However, cell physiological abnormalities caused by constitutively active RalA will be highly dependent on cell type. Which cell types are affected is dependent on whether RalGAPA1 is a major catalytic subunit of the RalGAP complex in the respective tissue because RalGAPA2
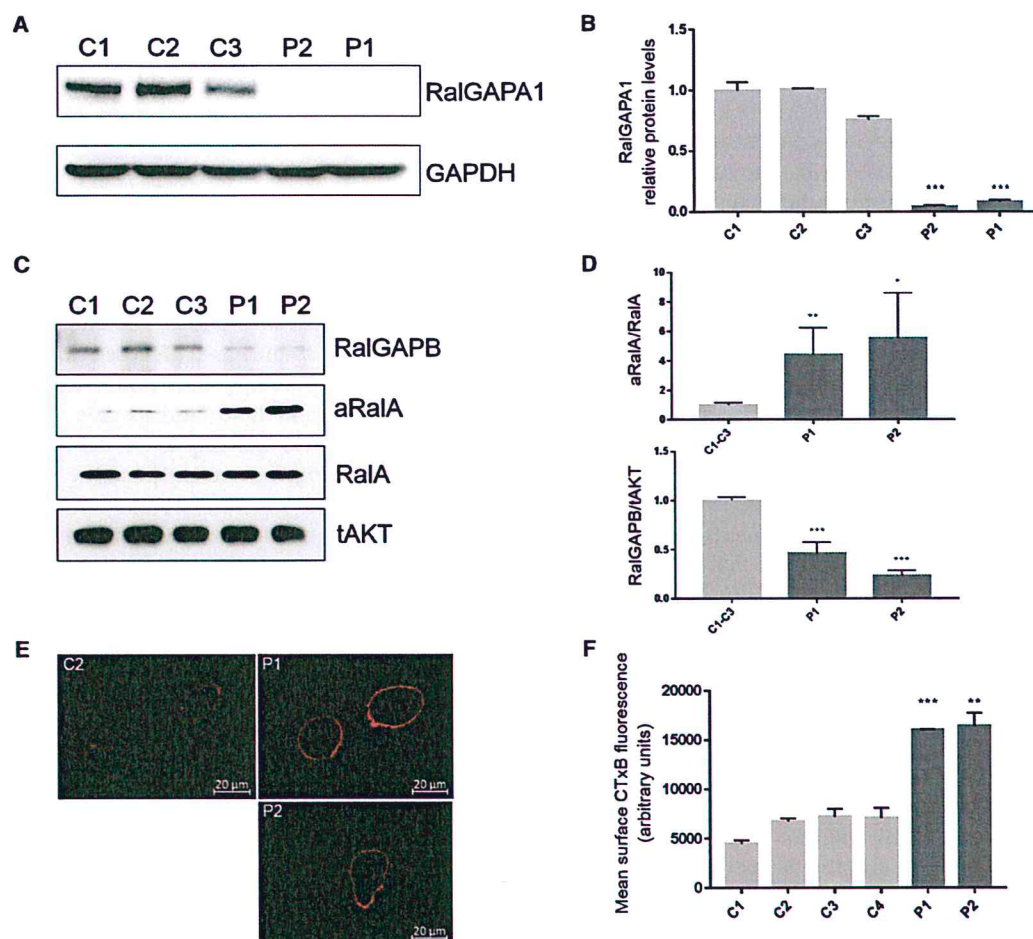
Figure 2. Functional Consequences of RalGAPA1 Deficiency

(A) Representative immunoblot image of fibroblasts derived from two individuals with pathogenic variants in *RALGAPA1* (P1 [derived from individual 1] and P2 [derived from individual 2]) and three control fibroblast lines (C1–C3). GAPDH served as a loading marker. Molecular weight: RalGAPA1 = 230 kDa; GAPDH = 36 kDa.

(B) Quantitated density of immunoblot bands from four independent experiments. Average values are presented as the mean ± SEM; ***p < 0.001 significantly different from controls. In P1 and P2 fibroblasts, RalGAPA1 levels are drastically reduced.

(C) Representative immunoblot image of active GTP-bound RalA (aRalA), which was determined by a pull-down assay with RalBP1 beads in comparison to RalGAPB, RalA, and tAKT levels. Molecular weight: RalGAPB = 165.2 kDa; RalA = 23.5 kDa; and AKT = 55.7 kDa.

(D) Quantification of immunoblot results from three independent experiments. Average values are presented as means ± SEM; *p < 0.05, **p < 0.01, and ***p < 0.001 significantly different from controls (C1–C3, pooled control). GTP-bound RalA levels are increased in P1 and P2 cell lines compared to controls (C1–C3). Moreover, protein levels of RalGAPB are reduced in P1 and P2 cell lines. The levels of AKT (AKT serine/threonine kinase 1) are not altered.

(E) Microscope images (optical sections) of CTxB Alexa 594 cell-surface fluorescence in detached human skin fibroblasts. Images were obtained with an Axio Observer Z1 microscope with ApoTome 2 (63× objective lens, Zeiss). Images depict typical examples of control fibroblasts (C2) and two fibroblast lines derived from affected individuals (P1 and P2).

(F) Quantification of CTxB Alexa 594 cell-surface fluorescence byFACS analysis. Results depicted represent data from three independent experiments. Average values are presented as means ± SEM; **p < 0.01 and ***p < 0.001 significantly different from controls. P1 and P2 fibroblasts show higher levels of CTxB Alexa 594 fluorescence, indicating a disturbance of lipid-raft clearance from the plasma membrane in detached cells.

might be predominant. In light of the above results, RalGAPA1 deficiency appears to have a crucial impact on neuronal function and development. Directly after birth, all individuals identified in this study displayed neuromuscular abnormalities (e.g., respiratory problems, feeding difficulties, muscular hypotonia) that later developed into severe psychomotor disability. Three individuals developed early-onset epilepsy. All children had mild-to-moderate dysmorphic facial features, and one had soft tissue syndactyly of fingers (see Figure 1 and Figure S9). Brain MRIs revealed dysplasia of the corpus callosum as well as additional variable CNS manifestations (e.g., gray-matter heterotopias, ectopic posterior pituitary) that suggested an impact on brain maturation (Figure 1 and Figures S2 and S3). Characterization of the *RALGAPA1* homolog in mice (*Ralgapa1*, also known as *GRIPE*) indicated that its

expression is upregulated in the developing brain during embryogenesis and remains high in the adult brain, especially in neurons of the cortex and hippocampus.[23] In addition, knockdown of the *RALGAPA1* homolog in zebrafish resulted in severe brain developmental delay.[12] Finally, RalGAPB knockout (which also leads to RalA activation) in mice is embryonic lethal (unpublished data). These data highlight the importance of *RALGAPA1* for neuronal development and differentiation.

On the basis of the complexity of the RalA pathway and its downstream effectors, the mechanisms behind the impact of disturbed RalA signaling on the nervous system will be difficult to dissect. Nevertheless, one important experimental result might be the disturbance that we observed in lipid-raft microdomains in RalGAPA1-deficient fibroblasts. It is well known that lipid remodeling is crucial for the development of the central nervous system via compartmentalization, signal transduction, cell adhesion, and axonal spreading.[24,25] Accordingly, altered lipid-raft trafficking might be a critical aspect of neuronal development in individuals with *RALGAPA1* variants.

Interestingly, the pathophysiology of RalGAPA1 deficiency might be at least in part similar to the mechanism of *RALA* variants published by Hiatt et al., 2018.[11] The majority of *RALA* variants cluster in the GDP/GTP binding pocket and are thus predicted to impair GDP/GTP binding. Three out of four *RALA* mutants that were tested in biochemical assays had a dramatic reduction in effector binding, and all mutants had a significantly reduced GTPase activity. The question of whether reduced effector binding together with decreased GTPase activity increases RalA signaling was not examined by the authors, but one *RALA* mutant was definitely constitutively activated, a finding similar to the RalA activation that we observed in RalGAPA1-deficient fibroblasts in this study. In general, the phenotype of the individuals with *RALA* variants was milder than in the children reported here. However, the core phenotype observed in individuals with variants in *RALGAPA1* resembles the phenotype of individuals with *RALA* variants in previous studies (e.g., this phenotype includes intellectual disability, developmental delay, muscular hypotonia, and early-onset epilepsy). Furthermore, facial abnormalities (e.g., a short nose, a flattened nasal bridge, and gingival hypertrophy) appear to be a common feature. In addition, more than half of the children reported as having *RALA* variants had a dysplastic corpus callosum (shortening/thinning), which appears to be also a unifying MRI feature in individuals with RalGAPA1 deficiency. Interestingly, in some of the individuals with *RALA* variants, finger abnormalities, as also seen in individual 3, were observed.[11] These striking similarities also pose an additional argument that *de novo* mutations in *RALA* might have the same downstream effect as the loss of *RALGAPA1*.

In light of the overlapping phenotype between *RALA*- and *RALGAPA1*-associated diseases, it becomes evident that dysregulation of the RalA signaling pathway leads to a distinct group of genetic syndromes that we suggest could be named RALopathies. This group of disorders could be expanded by the identification of further *RALA*-related disease genes.

In addition to the neurological disease manifestation, profound muscular hypotonia was a unifying clinical feature of affected individuals. This is of interest because RalA and the RalGAP complex have been implicated in the regulation of glucose uptake in response to insulin.[8] In mice, muscle-specific *Ralgapa1* deletion caused RalA activation, leading to increased glucose and the uptake of free fatty acids by muscles, thus improving whole body glucose handling and lipid homeostasis. However, the study did not address the impact of RalGAPA1 deletion on muscle physiology or contractile ability. Additionally, the genetic approach used in that study did not allow the authors to address the role of RalGAPA1 in muscle development because Cre recombinase under myosin light chain 1f promoter is expressed in mature muscle only. No abnormalities in glucose metabolism were identified in the children we report on here.

Another disease feature of RalGAPA1-deficient individuals was recurrent episodes of fever with or without viral infections, as was reported in three individuals. This might be related to the severe developmental disability (e.g., increased risk for infections as a result of immobility; risk of aspirations). However, fever episodes and viral infections started so early in life and occurred at such a high frequency that they triggered extensive immunological work-up in two of the individuals. In this context, it is important to note that the *RALGAPA1* homolog in mice binds E12, a transcriptional regulator of immunoglobulin genes.[23] Therefore, although no specific immune defect could be identified in the affected individuals, a possible role of *RALGAPA1* in immune function might be expected.

Finally, on the basis of the overactivation of RalA in autosomal-recessive RalGAPA1 deficiency, it is tempting to speculate that inhibition of the Ral pathway via the inhibition of Ral prenylation[26] or the phosphorylation of the Ral pathway by Aurora A or protein kinase C[27] might have a therapeutic effect. However, it will be very difficult to titrate the effect of such inhibitor approaches (especially against the background wherein RalA downregulation might also cause a neurological phenotype). Moreover, in light of the neonatal disease onset, it is suggestive that the variant already affects prenatal development in a way that might not be compensated for by a postnatal start of treatment. Further studies in knockout animal models of *RALGAPA1* will be helpful in addressing this issue.

Accession Numbers

The accession numbers for the data reported in this paper are as follows: for individual 1, ClinVar: VCV000691798 and VCV000691794; for individual 2, ClinVar: VCV000691795; for

individual 3, ClinVar: VCV000691796; and for individual 4, ClinVar: VCV000691797.

Supplemental Data

Supplemental Data can be found online at https://doi.org/10.1016/j.ajhg.2020.01.002.

Acknowledgments

Declaration of Interests

The authors declare no competing interests.

Web Resources

ClinVar, https://www.ncbi.nlm.nih.gov/clinvar/
GeneMatcher, https://www.genematcher.org
gnomAD Browser, https://gnomad.broadinstitute.org/
OMIM, https://www.omim.org/

References

1. Cooper, J.M., Bodemann, B.O., and White, M.A. (2013). The RalGEF/Ral pathway: evaluating an intervention opportunity for Ras cancers. The Enzymes *34 Pt. B*, 137–156.

2. Shirakawa, R., Fukai, S., Kawato, M., Higashi, T., Kondo, H., Ikeda, T., Nakayama, E., Okawa, K., Nureki, O., Kimura, T., et al. (2009). Tuberous sclerosis tumor suppressor complex-like complexes act as GTPase-activating proteins for Ral GTPases. J. Biol. Chem. *284*, 21580–21588.

3. Vigil, D., Cherfils, J., Rossman, K.L., and Der, C.J. (2010). Ras superfamily GEFs and GAPs: validated and tractable targets for cancer therapy? Nat. Rev. Cancer *10*, 842–857.

4. Ezzeldin, M., Borrego-Diaz, E., Taha, M., Esfandyari, T., Wise, A.L., Peng, W., Rouyanian, A., Asvadi Kermani, A., Soleimani, M., Patrad, E., et al. (2014). RalA signaling pathway as a therapeutic target in hepatocellular carcinoma (HCC). Mol. Oncol. *8*, 1043–1053.

5. Luo, J.Q., Liu, X., Frankel, P., Rotunda, T., Ramos, M., Flom, J., Jiang, H., Feig, L.A., Morris, A.J., Kahn, R.A., and Foster, D.A. (1998). Functional association between Arf and RalA in active phospholipase D complex. Proc. Natl. Acad. Sci. USA *95*, 3632–3637.

6. Ohta, Y., Suzuki, N., Nakamura, S., Hartwig, J.H., and Stossel, T.P. (1999). The small GTPase RalA targets filamin to induce filopodia. Proc. Natl. Acad. Sci. USA *96*, 2122–2128.

7. Peschard, P., McCarthy, A., Leblanc-Dominguez, V., Yeo, M., Guichard, S., Stamp, G., and Marshall, C.J. (2012). Genetic deletion of RALA and RALB small GTPases reveals redundant functions in development and tumorigenesis. Curr. Biol. *22*, 2063–2068.

8. Chen, Q., Quan, C., Xie, B., Chen, L., Zhou, S., Toth, R., Campbell, D.G., Lu, S., Shirakawa, R., Horiuchi, H., et al. (2014). GARNL1, a major RalGAP α subunit in skeletal muscle, regulates insulin-stimulated RalA activation and GLUT4 trafficking via interaction with 14-3-3 proteins. Cell. Signal. *26*, 1636–1648.

9. Sugihara, K., Asano, S., Tanaka, K., Iwamatsu, A., Okawa, K., and Ohta, Y. (2002). The exocyst complex binds the small GTPase RalA to mediate filopodia formation. Nat. Cell Biol. *4*, 73–78.

10. Leto, D., Uhm, M., Williams, A., Chen, X.W., and Saltiel, A.R. (2013). Negative regulation of the RalGAP complex by 14-3-3. J. Biol. Chem. *288*, 9272–9283.

11. Hiatt, S.M., Neu, M.B., Ramaker, R.C., Hardigan, A.A., Prokop, J.W., Hancarova, M., Prchalova, D., Havlovicova, M., Prchal, J., Stranecky, V., et al. (2018). De novo mutations in the GTP/GDP-binding region of RALA, a RAS-like small GTPase, cause intellectual disability and developmental delay. PLoS Genet. *14*, e1007671.

12. Shimojima, K., Komoike, Y., Tohyama, J., Takahashi, S., Páez, M.T., Nakagawa, E., Goto, Y., Ohno, K., Ohtsu, M., Oguni, H., et al. (2009). TULIP1 (RALGAPA1) haploinsufficiency with brain development delay. Genomics *94*, 414–422.

13. Schwarzbraun, T., Vincent, J.B., Schumacher, A., Geschwind, D.H., Oliveira, J., Windpassinger, C., Ofner, L., Ledinegg, M.K., Kroisel, P.M., Wagner, K., and Petek, E. (2004). Cloning, genomic structure, and expression profiles of TULIP1 (GARNL1), a brain-expressed candidate gene for 14q13-linked neurological phenotypes, and its murine homologue. Genomics *84*, 577–586.

14. DePristo, M.A., Banks, E., Poplin, R., Garimella, K.V., Maguire, J.R., Hartl, C., Philippakis, A.A., del Angel, G., Rivas, M.A., Hanna, M., et al. (2011). A framework for variation discovery and genotyping using next-generation DNA sequencing data. Nat. Genet. *43*, 491–498.

15. Li, M.X., Gui, H.S., Kwan, J.S., Bao, S.Y., and Sham, P.C. (2012). A comprehensive framework for prioritizing variants in exome sequencing studies of Mendelian diseases. Nucleic Acids Res. *40*, e53.

16. Alkuraya, F.S. (2013). The application of next-generation sequencing in the autozygosity mapping of human recessive diseases. Hum. Genet. *132*, 1197–1211.

17. Sobreira, N., Schiettecatte, F., Valle, D., and Hamosh, A. (2015). GeneMatcher: a matching tool for connecting investigators with an interest in the same gene. Hum. Mutat. *36*, 928–930.

18. Skorobogatko, Y., Dragan, M., Cordon, C., Reilly, S.M., Hung, C.W., Xia, W., Zhao, P., Wallace, M., Lackey, D.E., Chen, X.W., et al. (2018). RalA controls glucose homeostasis by regulating glucose uptake in brown fat. Proc. Natl. Acad. Sci. USA *115*, 7819–7824.

19. Saito, R., Shirakawa, R., Nishiyama, H., Kobayashi, T., Kawato, M., Kanno, T., Nishizawa, K., Matsui, Y., Ohbayashi, T.,

Horiguchi, M., et al. (2013). Downregulation of Ral GTPase-activating protein promotes tumor invasion and metastasis of bladder cancer. Oncogene *32*, 894–902.

20. Balasubramanian, N., Meier, J.A., Scott, D.W., Norambuena, A., White, M.A., and Schwartz, M.A. (2010). RalA-exocyst complex regulates integrin-dependent membrane raft exocytosis and growth signaling. Curr. Biol. *20*, 75–79.

21. Day, C.A., and Kenworthy, A.K. (2015). Functions of cholera toxin B-subunit as a raft cross-linker. Essays Biochem. *57*, 135–145.

22. Karczewski, K.J., Francioli, L.C., Tiao, G., Cummings, B.B., Alföldi, J., Wang, Q., Collins, R.L., Laricchia, K.M., Ganna, A., Birnbaum, D.P., et al. (2019). Variation across 141,456 human exomes and genomes reveals the spectrum of loss-of-function intolerance across human protein-coding genes. bioRxiv. https://doi.org/10.1101/531210.

23. Heng, J.I., and Tan, S.S. (2002). Cloning and characterization of GRIPE, a novel interacting partner of the transcription factor E12 in developing mouse forebrain. J. Biol. Chem. *277*, 43152–43159.

24. Olsen, A.S.B., and Færgeman, N.J. (2017). Sphingolipids: membrane microdomains in brain development, function and neurological diseases. Open Biol. *7*, 170069.

25. Tsui-Pierchala, B.A., Encinas, M., Milbrandt, J., and Johnson, E.M., Jr. (2002). Lipid rafts in neuronal signaling and function. Trends Neurosci. *25*, 412–417.

26. Berndt, N., Hamilton, A.D., and Sebti, S.M. (2011). Targeting protein prenylation for cancer therapy. Nat. Rev. Cancer *11*, 775–791.

27. Wu, J.C., Chen, T.Y., Yu, C.T., Tsai, S.J., Hsu, J.M., Tang, M.J., Chou, C.K., Lin, W.J., Yuan, C.J., and Huang, C.Y. (2005). Identification of V23RalA-Ser194 as a critical mediator for Aurora-A-induced cellular motility and transformation by small pool expression screening. J. Biol. Chem. *280*, 9013–9022.